



Synthesis and evaluation in vitro and in vivo of a ^{11}C -labeled cyclooxygenase-2 (COX-2) inhibitor

Frank Wuest*, Torsten Knies, Ralf Bergmann, Jens Pietzsch

Institute of Radiopharmacy, Research Center Dresden-Rossendorf, PO Box 510119, 01314 Dresden, Germany

ARTICLE INFO

Article history:

Received 17 March 2008

Revised 30 June 2008

Accepted 4 July 2008

Available online 10 July 2008

Keywords:

Positron emission tomography

Cyclooxygenase

COX-2 inhibitor

Carbon-11

Inflammation

Cancerogenesis

ABSTRACT

The radiosynthesis and radiopharmacological evaluation of 1- ^{11}C methoxy-4-(2-(4-(methanesulfonyl)phenyl)cyclopent-1-enyl)-benzene [^{11}C]5 as novel PET radiotracer for imaging of COX-2 expression is described. The radiotracer was prepared via *O*-methylation reaction with [^{11}C]methyl iodide in 19% decay-corrected radiochemical yield at a specific activity of 20–25 GBq/ μmol at the end-of-synthesis within 35 min. The radiotracer [^{11}C]5 was evaluated in vitro using various pro-inflammatory and tumor cell lines showing high functional expression of COX-2 at baseline or after induction. In vivo biodistribution of compound [^{11}C]5 was characterized in male Wistar rats. Compound [^{11}C]5 was rapidly metabolized in rat plasma, and more pronounced, in mouse plasma. In vivo kinetics and tumor uptake were demonstrated by dynamic small animal PET studies in a mouse tumor xenograft model. Tumor uptake of radioactivity was clearly visible overtime. However, radioactivity uptake in the tumor could not be blocked by the pre-injection of nonradioactive compound 5. Therefore, it can be concluded that radioactivity uptake in the tumor was not COX-2 mediated.

© 2008 Elsevier Ltd. All rights reserved.

1. Introduction

Cyclooxygenases (COXs) control the complex conversion of arachidonic acid to prostaglandins and thromboxanes, which trigger as autocrine and paracrine chemical messengers with many physiological and pathophysiological responses.^{1–3} The COXs exist in two distinct isoforms, a constitutive form (COX-1) and an inducible form (COX-2). More recently, a novel COX-1 splice variant termed as COX-3 has been reported.⁴ COX-1 and COX-2 share the same substrates, produce the same products, and catalyze the same reaction using identical catalytic mechanisms. The X-ray crystal structure of both enzymes suggests that the proteins are very similar in their tertiary conformation.^{5,6} The amino acids which serve as substrate binding pocket and catalytic site are nearly identical in both enzymes.^{7–9} The COX-1 enzyme is expressed in resting cells of most tissues, functions as a housekeeping enzyme, and is responsible for maintaining homeostasis (gastric and renal integrity) and normal production of eicosanes.¹⁰ COX-2 is predominantly found in brain and kidney while being virtually absent in most other tissues. However, COX-2 expression is significantly up-regulated as part of various acute and chronic inflammatory conditions. COX-2 expression can be induced in fibroblast, epithelial, endothelial, macrophage, and smooth muscle cells in response to growth factors, cytokines, and proinflammatory stimuli, and expression is usually transient.¹¹ Besides being associated with inflammation

and pain, it is well documented that especially COX-2 is overexpressed in many human cancer entities such as colorectal, gastric, and breast cancer.^{12,13} COX-2 enzyme is assumed to play an important role in carcinogenesis by stimulating angiogenesis, tissue invasion, metastasis, and apoptosis inhibition. COX-2 expression is stimulated by a number of inflammatory cytokines, growth factors, oncogenes, lipopolysaccharides, and tumor promoters.¹⁴

Since the discovery of the COX-2 enzyme in the early 1990s, much efforts have been made in the development of COX-2 selective inhibitors. Because of the structural similarities of the COX-1 and COX-2 enzyme, the search for selective inhibitors for COX-2 versus COX-1 represents a formidable challenge. Based on the common diaryl heterocycle platform, as initially described for DuP 697 as a COX-2 selective inhibitor, a large array of different compounds has been reported as selective COX-2 inhibitors. A selection of different selective COX-2 inhibitors, such as DuP 697, celecoxib, rofecoxib, and valdecoxib, is depicted in Figure 1.

Currently, an exact and accurate assessment of COX-2 expression levels and/or activity in organs or tissues can only be achieved by laborious analyses ex vivo. Moreover, instability of COX-2 mRNA and protein leads to further difficulties in terms of the intervals between tissue sampling and time of analysis. In this line, non-invasive monitoring of COX-2 functional expression by means of nuclear molecular imaging techniques like positron emission tomography (PET) and single photon emission computed tomography (SPECT) provides unique opportunities to obtain data on COX-2 expression levels during disease progression and the potential role of COX-2 in diseases. Moreover, the development and in vivo

* Corresponding author. Tel./fax: +49 351 260 27 60.

E-mail address: f.wuest@fz-rossendorf.de (F. Wuest).

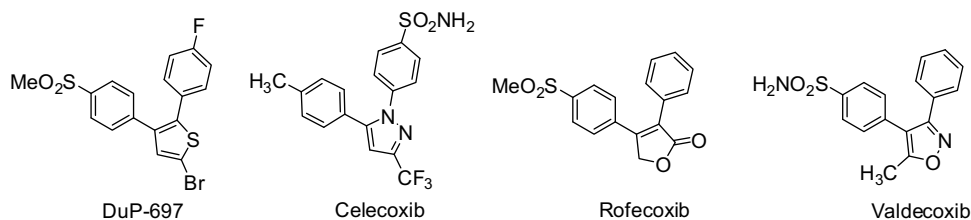


Figure 1. Selection of selective COX-2 inhibitors.

study of appropriately radiolabeled selective COX-2 inhibitors would provide pharmacological data, which may help to understand their exact physiological actions and metabolic pathways.

Over the last decade, various attempts have been made to develop radiotracers for COX-2 imaging with PET and SPECT. As a result, several ^{18}F - and ^{11}C -labeled analogues of DuP-697,¹⁵ celecoxib,^{16,17} rofecoxib,^{18–20} valdecoxib,^{18,21} and other compounds containing a heterocycle core structure^{22–24} have been synthesized and, in some cases, radiopharmacologically evaluated in vivo as potential PET radiotracers for imaging of COX-2. Moreover, some reports have also described the synthesis of $^{99\text{m}}\text{Tc}$ - and ^{123}I -labeled analogues of celecoxib^{25,26} as potential SPECT imaging agents. However, all reports have revealed that to date no satisfactory nuclear probe for in vivo imaging of COX-2 expression is available.

Recently, various 1,2-diarylcyclopentenes have been reported as high affinity and selective COX-2 inhibitors.^{27,28} The determined IC_{50} values in a COX-2 enzyme binding assay were in the low nanomolar range while showing high COX-1/COX-2 selectivity ratios favoring binding toward the COX-2 enzyme. Among various 1,2-diarylcyclopentenes as selective COX-2 inhibitors, compounds containing a 4-methoxyphenyl substituent showed especially high affinity and selectivity toward the COX-2 enzyme (Fig. 2).²⁸

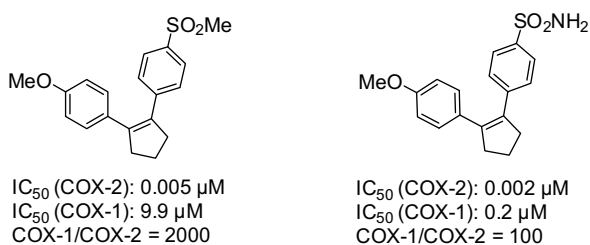


Figure 2. High affinity selective COX-2 inhibitors containing a cyclopentene core structure.²⁸

Both compounds possess high affinity for COX-2, and especially the compound containing a methyl sulfone substitution pattern shows a favorable COX-1/COX-2 selectivity profile (COX-2/COX-1 ratio: 2000). Moreover, the methoxy group makes this compound especially attractive for isotopic labeling with the short-lived positron emitter ^{11}C ($t_{1/2} = 20.4$ min) through a methylation reaction of the corresponding desmethyl precursor with [^{11}C]methyl iodide.

Here, we report on the radiosynthesis and radiopharmacological evaluation of 1-[^{11}C]methoxy-4-(2-(4-(methanesulfonyl)phenyl)cyclopent-1-enyl)-benzene ([^{11}C]5) as potential nuclear imaging probe for monitoring COX-2 expression in vivo by means of PET. The radiopharmacological characterization of [^{11}C]5 involved cell uptake studies, metabolism and biodistribution studies in normal rats, and small animal PET studies in NMRI nu/nu mice bearing the human colorectal adenocarcinoma tumor HT-29.

2. Results

2.1. Chemistry and radiochemistry

The synthesis of the appropriate desmethyl compound **6** as the labeling precursor for incorporating the ^{11}C label and substance **5** as the reference compound is given in Figure 3.

The synthesis of 1,2-diarylcyclopentenes was conveniently carried out via sequential Suzuki cross-coupling reactions starting from commercially available 1,2-dibromocyclopentene **1**. The sequential Suzuki cross-coupling reactions were performed in a bi-layer system (toluene/ Na_2CO_3 -solution) at elevated temperatures using commercially available boronic acids **2** and **4** as the coupling partners, and $\text{Pd}(\text{PPh}_3)_4$ as the catalyst. In the first step of the reaction sequence, the 4-methoxyphenyl substituent was introduced. For this purpose, two equivalents of 1,2-dibromocyclopentene **1** were used in the cross-coupling reaction with 4-methoxyphenyl boronic acid **2** to minimize the formation of the corresponding symmetrically bis-coupled product. Following this procedure, the mono-substituted cross-coupling product **3** could be isolated in

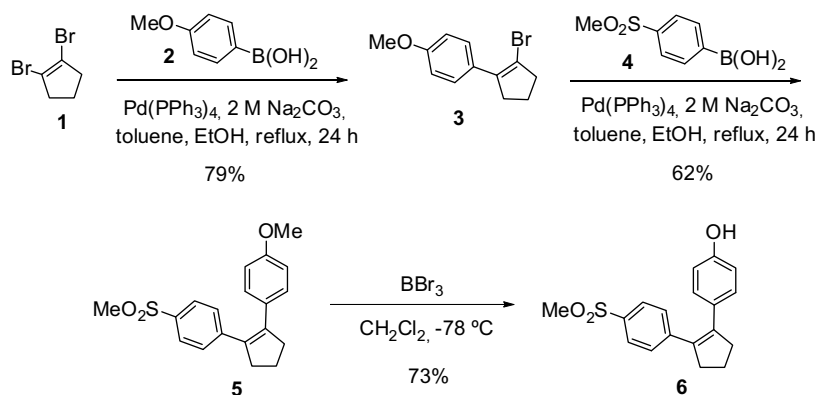


Figure 3. Synthesis of labeling precursor **6** and reference compound **5**.

79% yield after purification by means of flash chromatography. A second Suzuki cross-coupling reaction of equimolar amounts of mono-substituted compound **3** with 4-(methylsulfonyl)phenyl boronic acid **4** afforded the desired 1,2-diaryl cyclopentene **5** as the reference compound in 62% isolated yield. Standard treatment of compound **5** with BBr_3 in methylene chloride at -78°C led to cleavage of the methoxy group resulting in the formation of compound **6** as the desired labeling precursor in 73% isolated yield.

The radiosynthesis of compound $[^{11}\text{C}]\mathbf{5}$ was accomplished through an *O*-methylation reaction of desmethyl precursor **6** with $[^{11}\text{C}]\text{methyl iodide}$ in a remotely controlled synthesis module (Fig. 4).

$[^{11}\text{C}]\text{Methyl iodide}$ was transferred in a stream of nitrogen into the reaction vessel containing the sodium salt of desmethyl precursor **6** in DMF and 5 N NaOH at -20°C . The formation of the sodium salt of compound **6** could easily be monitored by the appearance of a yellow color. After completion of the $[^{11}\text{C}]\text{MeI}$ transfer, the reaction vessel was sealed and heated at 60°C for 3 min. The reaction mixture was diluted with eluent, and the mixture was transferred from the reaction vessel onto a semi-preparative C-18 column. The fraction eluting at 8–9 min was collected, diluted with water, and passed through a C-18 Sep-Pak Light cartridge. The cartridge was washed with water and the desired radiotracer $[^{11}\text{C}]\mathbf{5}$ was eluted with ethanol. Addition of 0.9% saline gave a final 5% EtOH solution of compound $[^{11}\text{C}]\mathbf{5}$ in saline suitable for subsequent *in vitro* and *in vivo* experiments. Radiotracer $[^{11}\text{C}]\mathbf{5}$ was obtained in a radiochemical yield of 19% (decay-corrected, based upon $[^{11}\text{C}]\text{CO}_2$) after HPLC purification at a specific radioactivity of 20–25 GBq/ μmol at the end-of-synthesis within 35 min. The radiochemical purity exceeded 95%.

2.2. Cell uptake studies

Several human and murine cell lines were used to study the uptake of compound $[^{11}\text{C}]\mathbf{5}$ *in vitro*. All cell lines used show constitutive expression of COX-1. To differentiate between the specific contribution of COX-1 and COX-2 to overall tracer uptake and intracellular association, unstimulated human (THP-1) and murine (RAW 264.7) monocytes/macrophages and quiescent murine fibroblasts (NIH 3T3) were used as models showing very low baseline expression of COX-2.^{29–31} In contrast, human tumor cell lines FaDu and HT29, respectively, mouse (fibroblast-like) preadipocytes (3T3 L1) and both TPA-stimulated THP-1 and RAW 264.7 cells served as models for upregulated COX-2 expression.^{30,32–34} The specificity of the radiotracer uptake was further tested by performing blocking experiments with all cells after preincubation with a 100 $\mu\text{mol/L}$ solution of the corresponding nonradioactive reference compound **5** for 10 min (Fig. 5).

2.3. Biodistribution in normal rats

The distribution of radioactivity in selected tissues and organs was studied in normal Wistar rats at two different time points (5 and 60 min) after injection of $[^{11}\text{C}]\mathbf{5}$. The results are depicted in Table 1.

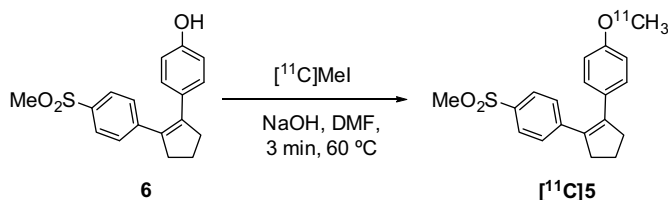


Figure 4. Radiosynthesis of COX-2 inhibitor $[^{11}\text{C}]\mathbf{5}$.

High radioactivity uptake was found in the liver, pancreas, and white adipose tissue. Moreover, the radiotracer seems readily to penetrate the blood–brain barrier as shown by the high initial brain uptake of $0.59 \pm 0.07\% \text{ID/g}$ at 5 min after radiotracer injection. Except for white adipose tissue, radioactivity was cleared from all organs and tissues within 60 min after radiotracer administration. The determined biodistribution profile suggests a hepatobiliary elimination of the radiotracer, and the overall tissue distribution of compound $[^{11}\text{C}]\mathbf{5}$ is consistent with the high lipophilicity of the radiotracer ($\log P = 4.2$) as determined on the basis of ACDLab[®] predictions.

2.4. Metabolite analysis

Metabolite analysis of arterial blood samples with radio-HPLC indicated that compound $[^{11}\text{C}]\mathbf{5}$ was rapidly metabolized to a single more polar metabolite in rat and mouse plasma. Metabolism of compound $[^{11}\text{C}]\mathbf{5}$ in mouse plasma was significantly more rapid compared with metabolism in rat plasma. The amount of the polar metabolite steadily increased overtime. Conversely, the amount of intact compound $[^{11}\text{C}]\mathbf{5}$ decreased, being 97% at 1 min, 57% at 5 min, 35% at 10 min, 26% at 20 min, 22% at 30 min, and 18% at 60 min in rat plasma, and 95% at 1 min, 40% at 5 min, 17% at 10 min, 8% at 20 min, 5% at 30 min, and 2% at 60 min in mouse plasma (Fig. 6).

2.5. *In vivo* small animal PET imaging in HT-29 tumor-bearing mice

To further assess the feasibility of compound $[^{11}\text{C}]\mathbf{5}$ as a PET radiotracer for imaging COX-2 expressing tumors, small animal PET imaging was performed in tumor-bearing mice. In the small animal PET experiments, 30 MBq of $[^{11}\text{C}]\mathbf{5}$ was administered intravenously over 1 min into the tail vein of NMRI nu/nu mice bearing human colorectal adenocarcinoma tumor HT-29.³⁵ This equals a total amount of 2–3 μg of compound **5**.

PET imaging was performed over 60 min with a dedicated small animal PET scanner (microPET[®] P4, Siemens CTI Molecular Imaging Inc., Knoxville) to elucidate the *in vivo* biodistribution of compound $[^{11}\text{C}]\mathbf{5}$ overtime, and to assess accumulation of radioactivity in the xenotransplanted HT-29 tumor. Figure 7 shows two representative PET images of radioactivity distribution at 1 and 50 min after radiotracer administration.

Accumulation of radioactivity in the HT-29 xenografted tumor over time was clearly visible. However, attempts to block uptake in the tumor by pre-injection with nonradioactive compound **5** proved to be unsuccessful. No decrease in radioactivity accumulation was observed (data not shown).

Time–activity curves representing time–activity concentration were used to further assess the kinetics of $[^{11}\text{C}]\mathbf{5}$ in blood (corrected for metabolites), muscle, and tumor. The time–activity curves and the derived increasing tumor-to-muscle ratio are shown in Figure 8.

The obtained time–activity curves confirm rapid clearance of the radiotracer from the blood and muscle, whereas accumulation of radioactivity was observed in the tumor until 10 min *p.i.*, followed by a slow wash out of radioactivity from tumor tissue. The tumor-to-muscle ratio is increasing overtime, reaching 1.7 at 60 min after radiotracer injection.

3. Discussion

Among the plethora of different COX-2 inhibitors developed during the last 15–20 years, most compounds share a common 1,2-diaryl heterocycle structure motif as exemplified for the approved selective COX-2 inhibitors celecoxib (Celebrex), rofecoxib (VIOXX), and valdecoxib (Bextra).

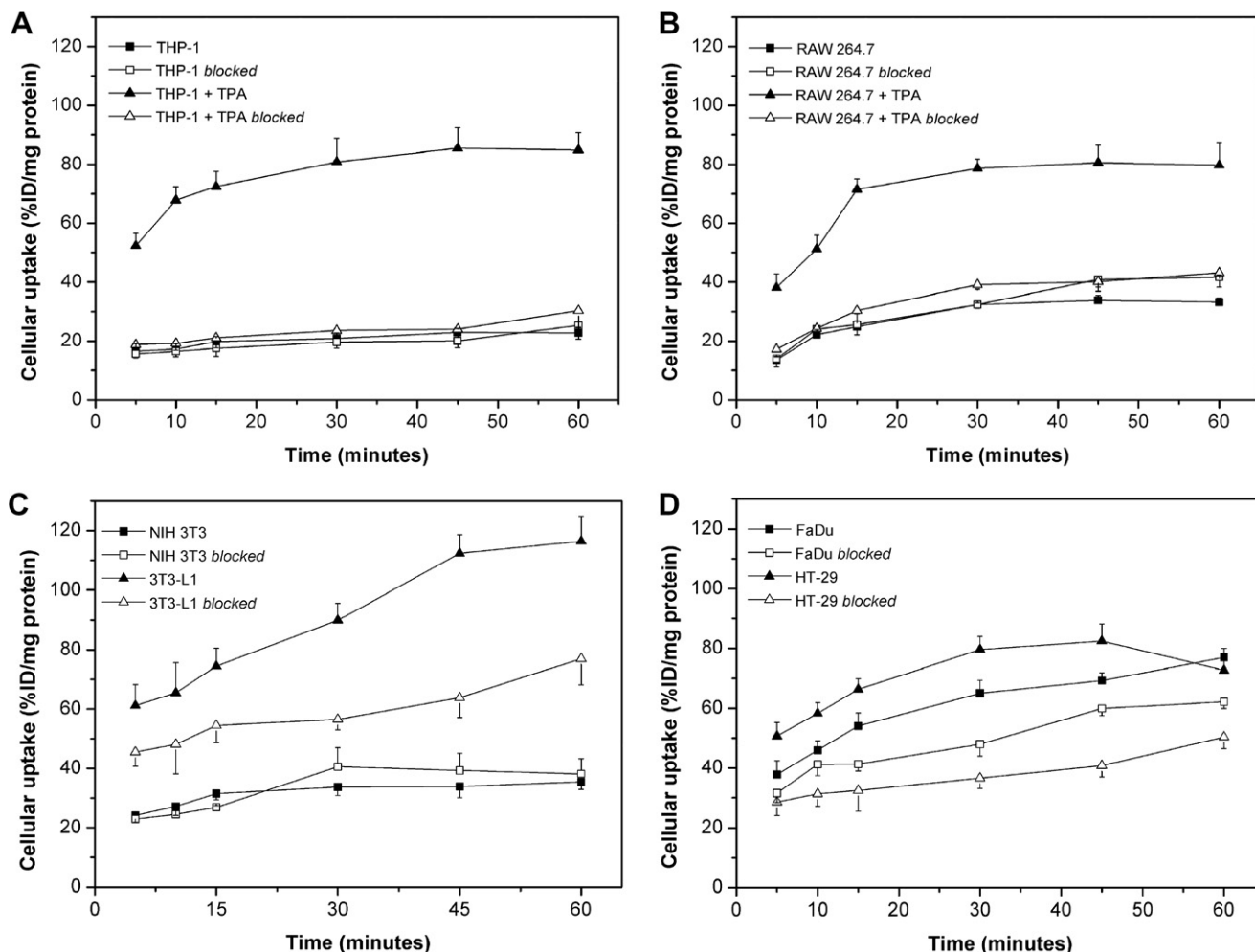


Figure 5. In vitro study on cellular uptake and intracellular association of compound $[^{11}\text{C}]\mathbf{5}$ in human monocytes/macrophages (A), murine monocytes/macrophages (B), murine fibroblasts/fibroblast-like cells (C), and human tumor cells (D). Results are given as mean \pm SD ($n = 4$). TPA, stimulation by 64 nM phorbol myristate acetate (TPA) for 72 h; *blocked*, preincubation (for 10 min) with a 100 $\mu\text{mol/L}$ solution of the corresponding nonradioactive reference compound **5**.

Table 1
Biodistribution of $[^{11}\text{C}]\mathbf{5}$ in selected tissues and organs of normal male Wistar rats (body weight 179 ± 10 g) after single intravenous application at 5 min and 60 min p.i. Data are presented as %ID/g, mean \pm SD (4 animals per time point)

Time p.i.	5 min	60 min
Blood	0.23 ± 0.08	0.18 ± 0.03
Brain	0.59 ± 0.07	0.11 ± 0.01
Heart	0.50 ± 0.04	0.16 ± 0.03
Lung	0.59 ± 0.09	0.19 ± 0.01
Liver	1.35 ± 0.25	0.76 ± 0.12
Spleen	0.32 ± 0.04	0.21 ± 0.01
Pancreas	0.78 ± 0.12	0.52 ± 0.01
Adrenals	1.33 ± 0.11	0.57 ± 0.06
Kidneys	0.62 ± 0.06	0.26 ± 0.01
Thymus	0.64 ± 0.13	0.20 ± 0.04
Muscle	0.32 ± 0.05	0.11 ± 0.01
Harderian glands	1.06 ± 0.30	0.42 ± 0.07
Brown adipose tissue	1.89 ± 0.65	0.67 ± 0.18
White adipose tissue	0.53 ± 0.29	0.52 ± 0.09
Femur	0.34 ± 0.06	0.19 ± 0.05
Testes	0.20 ± 0.03	0.09 ± 0.01

The basic 1,2-diaryl heterocycle platform was used for various structural modifications leading to COX inhibitors with a high selectivity profile toward the COX-2 enzyme. In this line, a methyl sulfone or sulfonamide substitution pattern attached to one of the

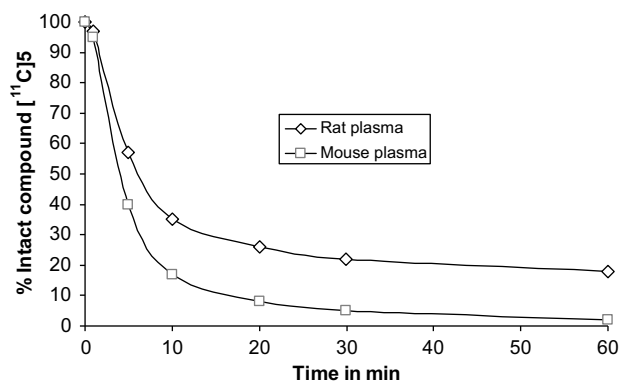


Figure 6. Intact compound $[^{11}\text{C}]\mathbf{5}$ overtime in rat plasma (diamonds) and mouse plasma (squares).

aryl substituents proved to be essential for a favorable high selectivity ratio COX-2 versus COX-1.³⁶ Consequently, the development of radiotracers for imaging COX-2 expression in vivo was also mainly focused on compounds containing a central heterocyclic core structure. The preferred radioisotopes for radiolabeling were the short-lived positron emitters ^{11}C ($t_{1/2} = 20.4$ min) and ^{18}F ($t_{1/2} = 109.8$ min). Radiosyntheses were accomplished either by using one

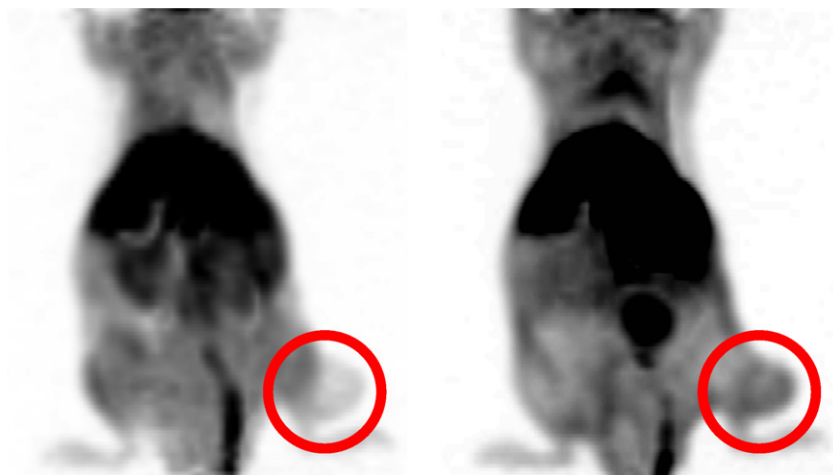


Figure 7. Representative coronal small animal PET images (maximum intensity projection) of HT-29 tumor (red circle)-bearing mice 1 min (left) and 50 min (right) after single intravenous application of 30 MBq of [^{11}C]5.

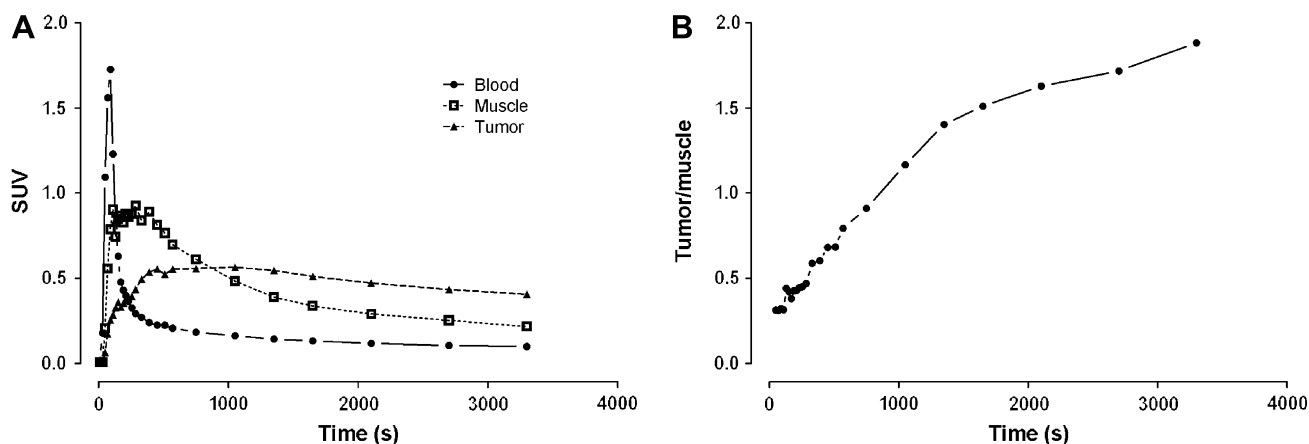


Figure 8. Representative time-activity curves from one animal after single intravenous application of [^{11}C]5. (A) Time-activity concentration (SUV) curves of the blood (corrected for metabolites), tumor and muscle. (B) Increasing tumor-to-muscle ratio over time.

of the aryl substituents or by utilizing the central heterocycle moiety as the preferred sites for the incorporation of the radiolabel.

Besides numerous COX-2 selective inhibitors containing a central heterocyclic core structure, various 1,2-diarylcyclopentenes, as depicted in Figure 2, also showed a remarkable high affinity and selectivity toward the COX-2 enzyme.^{27,28} In particular, the high affinity and selectivity of methyl sulfone-containing compound **5** toward COX-2 within the array of 1,2-diarylcyclopentene-containing compounds prompted us to set up a radiosynthesis of the corresponding ^{11}C -labeled radiotracer [^{11}C]5. The radiosynthesis was based on standard methylation reaction of desmethyl precursor **6** with readily available [^{11}C]methyl iodide. The required labeling precursor **6** and the reference compound **5** were easily prepared through two consecutive Suzuki cross-coupling reactions starting from commercially available 1,2-dibromocyclopentene. The used reaction sequence for the synthesis of compounds **5** and **6** differs significantly from the procedure reported in the literature. The literature procedure requires an additional oxidation step of a methyl thioether intermediate to give the desired monosubstituted methyl sulfone as the coupling partner for the second Suzuki cross-coupling reaction.²⁸

We found that the choice of the aryl boronic acid to be attached first onto the cyclopentene ring via Suzuki reaction proved to be very important for the success of the entire reaction. Hence, when

4-(methyl-sulfonyl)phenyl boronic acid **4** was used as the coupling partner in the first Suzuki cross-coupling step, only the undesired symmetrically bis-coupled product could be isolated, even when an excess of 1,2-dibromocyclopentene **1** was used. Conversely, the use of 4-methoxyphenyl boronic acid **2** as the coupling partner in the first Suzuki cross-coupling step with 1,2-dibromocyclopentene **1** gave nicely the desired monosubstituted intermediate **3** in good isolated 79% yield. Intermediate **3** could easily be converted into compound **5**, which was further reacted to give the labeling precursor **6**. Compounds **5** and **6** were obtained in total chemical yields of 49% and 36%, respectively.

The radiosynthesis of [^{11}C]5 was performed in a remotely controlled synthesis apparatus (Nuclear Interface, Münster), which allowed the convenient and reproducible performance of the radiolabeling reaction. [^{11}C]Methyl iodide was prepared starting from [^{11}C]CO₂ according to the 'wet' chemistry route.³⁷ Radiolabeling was easily carried out by standard treatment of desmethyl precursor **6** with [^{11}C]methyl iodide. In a typical experiment 60 GBq of [^{11}C]CO₂ could be converted into 3.5 GBq of [^{11}C]5 (19% decay-corrected radiochemical yield, based upon [^{11}C]CO₂) after HPLC purification within 35 min. The radiochemical purity exceeded 95%. The obtained specific radioactivity of 20–25 GBq/ μmol equals a total amount of 4.5 to 6 $\mu\text{g}/\text{ml}$ of cold compound **5** in the final product solution.

Cellular uptake studies revealed a comparable moderate uptake of compound [^{11}C]5 in all cells showing no or only very low baseline expression of COX-2. In these cells radiotracer uptake was not influenced by preincubation with the nonradioactive reference compound 5. On the other hand, in cells showing high baseline expression of COX-2 (HT-29, FaDu, and 3T3 L1) or TPA-stimulated COX-2 expression (THP-1 and RAW 264.7), respectively, overall radiotracer uptake and intracellular association was markedly higher. This increment in overall radiotracer uptake and intracellular association could be substantially reduced by pre-incubation of the cells with a molar excess of the nonradioactive reference compound 5, indicating high specificity of compound [^{11}C]5 for COX-2 in vitro. Of note, the tumor promoter TPA (12-*O*-tetradecanoylphorbol-13-acetate) used in the present study was reported to act as a potent inducer of COX-2 expression in various cell types, particularly, macrophages and monocytic cells.³⁸

In the biodistribution study in normal rats, the radiotracer [^{11}C]5 showed clearance from all tissues and organs within the time frame studied, except for white adipose tissue. The radiotracer showed a 22% clearance from the blood at 60 min p.i. reaching $0.18 \pm 0.03\text{ID/g}$. The remaining radioactivity concentration of $0.18 \pm 0.03\text{ID/g}$ in the blood at 60 min after radiotracer administration is in agreement with the observed radioactivity concentration of other ^{11}C -labeled²⁴ and ^{18}F -labeled COX-2 inhibitors¹⁶, whereas a ^{125}I -labeled³⁹ and one other ^{11}C -labeled COX-2 inhibitor²⁴ showed a higher radioactivity concentration in the blood of 0.44% and 1.16%ID/g, respectively, at 60 min p.i. The highest initial radioactivity uptake after 5 min p.i. of compound [^{11}C]5 was observed in the brown adipose tissue ($1.89 \pm 0.65\text{ID/g}$), liver ($1.35 \pm 0.25\text{ID/g}$), adrenals ($1.33 \pm 0.11\text{ID/g}$), and Harderian glands ($1.06 \pm 0.30\text{ID/g}$). Compared to other tissues and organs, relatively high initial radioactivity concentration was further found in the pancreas ($0.78 \pm 0.12\text{ID/g}$ at 5 min p.i.). The clearance of radioactivity in the pancreas was lower (33%) compared to other tissues and organs with high initial radiotracer uptake (64% for brown adipose tissue; 44% for liver, and 57% for adrenals).

The radiotracer seems to readily penetrate the blood–brain barrier resulting in an initial radioactivity concentration in the brain of $0.59 \pm 0.07\text{ID/g}$ after 5 min p.i. However, this initial high brain uptake decreased significantly to $0.11 \pm 0.01\text{ID/g}$ after 60 min p.i. representing an 80% clearance. Although the brain is known as an organ where COX-2 is constitutively expressed, in our study only little retention of radioactivity was found in the brain after 60 min p.i. This finding is consistent with other reports in the literature showing also only little radioactivity concentration (0.04% to 0.15%ID/g) in the brain at 60 min after radiotracer administration for other ^{11}C -labeled COX-2 inhibitors.²⁴ The kidneys are also known to express COX-2 at high levels.⁴⁰ However, radioactivity concentration in the kidney was rapidly cleared overtime, being $0.62 \pm 0.06\text{ID/g}$ at 5 min p.i. and $0.26 \pm 0.01\text{ID/g}$ at 60 min p.i. The observed kidney clearance agrees with results reported in the literature using other ^{11}C -labeled COX-2 inhibitors.²⁴

Metabolite analysis of arterial blood samples from rat and mouse showed that compound [^{11}C]5 was rapidly metabolized. The fast metabolism of the radiotracer was more pronounced in mice, leading to a fraction of intact parent compound in mouse plasma as little as 17% at 10 min after radiotracer administration. In mice, compound [^{11}C]5 was almost completely metabolized at later time points, resulting in only 8% of intact radiotracer at 20 min, 5% at 30 min, and 2% at 60 min. The fast metabolism of the radiotracer suggests the incorporation of the radiolabel into a different, metabolically more stable position of the molecule. In this line, the methylsulfone moiety represents an alternative functional group suitable for the incorporation of ^{11}C via a methylation reaction with [^{11}C]methyl iodide. The radiosynthesis of corre-

sponding [^{11}C]methylsulfones could easily be performed either via a two-step in situ deprotection/methylation oxidation procedure¹⁹ or via a direct labeling strategy with [^{11}C]methyl iodide starting from the corresponding sulfinate precursor.²⁰

Dynamic small animal PET studies using compound [^{11}C]5 in a mouse HT-29 tumor xenograft model revealed accumulation in the xenotransplanted tumor. Radioactivity accumulation in the tumor peaked at 10 min followed by a slow wash-out within the time frame of the study. The accumulation of radioactivity in the tumor was further confirmed by an increasing tumor-to-muscle ratio overtime. This observation is consistent with our data showing comparably high uptake of compound [^{11}C]5 in HT-29 cells in vitro. The human colorectal adenocarcinoma cell line HT-29 was used as a well characterized model showing increased baseline levels of COX-2 mRNA and protein.^{41–46} However, intraperitoneal injection of nonradioactive COX-2 inhibitor 5 at a dose of 5 mg/kg body weight 10 min prior to radiotracer administration to block radiotracer uptake in the tumor and to confirm a COX-2-mediated uptake in vivo was not successful probably due to the too low COX-2 expression in the HT-29 xenotransplanted tumor. Application of higher doses of compound 5 (>5 mg/kg), as well as an intravenous administration of the blocking agent, was not possible due to solubility problems. Hence, the need for an intraperitoneal administration and the use of 5 mg/kg as blocking dose presumably resulted in limited bioavailability and low total amount of compound 5 to sufficiently block radioactivity uptake in the tumor. The failure of blocking of radioactivity uptake in the xenografted tumor is in contrast to the cellular uptake studies in vitro. However, in these studies a much higher concentration (100 $\mu\text{mol/L}$) of compound 5 as blocking agent was used. The overall organ-specific in vivo distribution of compound [^{11}C]5 in mice as observed in the small animal PET studies was comparable with the results from the biodistribution studies in rats.

4. Conclusion

In this report, we have described the radiosynthesis and radiopharmacological evaluation of a ^{11}C -labeled COX-2 inhibitor containing a 1,2-diarylcyclopentenes structure as a novel lead for COX-2 selective PET radiotracers. Radiotracer [^{11}C]5 was fully characterized in vitro and in vivo, revealing rapid metabolism in rat plasma, and more pronounced, in mouse plasma. The high metabolic degradation of compound [^{11}C]5 in the animal experiments and the different COX-2 expression patterns in the in vivo and in vitro experiments may explain the large differences of the results obtained in vitro and in vivo. In terms of radiotracer metabolism, introduction of the ^{11}C label into the methylsulfone group should be envisaged to improve the metabolic profile of the radiotracer. The in vitro results indicate that compound [^{11}C]5 may have the potential as a COX-2 PET radiotracer to allow the quantification of COX-2 expression related to tumorigenic processes, for example, in colorectal cancer. However, the contribution of tumor cells and proinflammatory cells like macrophages to the overall uptake of compound [^{11}C]5 in tumors, tumor environment and/or inflammatory lesions has still to be further elucidated. Moreover, for further studies of COX-2 expression in vivo, compounds with higher affinity in combination with very high-specific activity should be developed.

5. Experimental

5.1. General

All commercial reagents and solvents were used without further purification unless otherwise specified. Nuclear magnetic resonance spectra were recorded on a Varian Unity 300 MHz spectrometer.

¹H-NMR chemical shifts were given in ppm and were referenced with the residual solvent resonances relative to tetramethylsilane (TMS). Mass spectra were obtained on a Quattro/LC mass spectrometer (MICROMASS) by electrospray ionization.

Flash chromatography was conducted according to Still et al.⁴⁷ using MERCK silica gel (mesh size 230–400 ASTM). Thin-layer chromatography (TLC) was performed on Merck silica gel F-254 aluminum plates with visualization under UV (254 nm).

5.2. Chemical synthesis

5.2.1. 1-(2-Bromocyclopent-1-enyl)-4-methoxybenzene (3)

To a solution of 1,2-dibromocyclopentene **1** (1.0 g, 4.40 mmol) and 4-methoxyphenyl boronic acid **2** (336.3 mg, 2.20 mmol) in toluene (30 mL), EtOH (30 mL), and 2 M Na₂CO₃ (30 mL) was added Pd(PPh₃)₄ (127.2 mg, 0.11 mmol). The mixture was refluxed overnight under a nitrogen atmosphere. After the addition of water (250 mL) the mixture was extracted with EtOAc. The solvent was evaporated and the residue was purified by flash chromatography (50% EtOAc/petrol ether) to give 440 mg (79% based upon 4-(methoxyphenyl boronic acid) of compound **3** as an oil. ¹H NMR (CDCl₃, 400 MHz): δ 2.06 (quint., *J* = 7.6 Hz, 2H, CH₂). 2.74 (t, *J* = 7.6 Hz, 2H, CH₂). 2.85 (t, *J* = 7.6 Hz, 2H, CH₂). 3.82 (s, 3H, CH₃). 6.90 and 7.58 (2d of AA'BB' system, *J* = 8.8 Hz, 4H, Ar-H).

5.2.2. 1-Methoxy-4-(2-(4-(methanesulfonyl)phenyl)cyclopent-1-enyl)-benzene (5)

To a solution of 1-(2-bromocyclopent-1-enyl)-4-methoxybenzene **3** (375 mg, 1.48 mmol) and 4-(methylsulfonyl)phenyl boronic acid **4** (296 mg, 1.48 mmol) in toluene (20 mL), ethanol (20 mL), and 2 M Na₂CO₃ (20 mL) was added Pd(PPh₃)₄ (87 mg, 0.075 mmol). The mixture was refluxed for 8 h under a nitrogen atmosphere. After the addition of water (150 mL), the mixture was extracted with EtOAc. After removal of the solvent under reduced pressure, the residue was purified by flash chromatography (50% EtOAc/petrol ether) to give 300 mg (62%) of the desired product **5** as a solid. Mp 128–130 °C; ¹H NMR (CDCl₃, 400 MHz): δ 2.07 (quint., *J* = 7.3 Hz, 2H, CH₂). 2.89 (t, *J* = 7.3 Hz, 4H, CH₂). 3.04 (s, 3H, CH₃), 3.79 (s, 3H, CH₃). 6.77 and 7.07 (2d of AA'BB' system, *J* = 8.8 Hz, 4H, Ar-H). 7.35 and 7.75 (2d of AA'BB' system, *J* = 8.5 Hz, 4H, Ar-H). Low-resolution mass spectrometry electron-spray ionization (ESI+): 351.4 [M+Na].

5.2.3. 4-[2-(4-Methanesulfonyl-phenyl)-cyclopent-1-enyl]-phenol (6)

1-Methoxy-4-(2-(4-(methane-sulfonyl)phenyl)cyclopent-1-enyl)-benzene **5** (170 mg, 0.52 mmol) was dissolved in dry methylene chloride (2 mL). The solution was cooled to –78 °C and 1 M BBr₃ solution in methylene chloride (0.6 mL, 0.6 mmol) was added. The resulting brown-colored solution was warmed up to ambient temperature and stirring was continued for 1 h. The solution was re-cooled to –78 °C and MeOH (1 mL) was added. The green solution was stirred for an additional hour at 0 °C. The solvent was evaporated, and the residue was purified by flash chromatography (40% EtOAc/petrol ether) to give 120 mg (73%) of the desired compound **6** as a solid. Mp 154–156 °C; ¹H NMR (CDCl₃, 400 MHz): δ 2.07 (quint., *J* = 7.3 Hz, 2H, CH₂). 2.89 (t, *J* = 7.3 Hz, 4H, CH₂). 3.04 (s, 3H, CH₃). 6.70 and 7.03 (2d of AA'BB' system, *J* = 8.3 Hz, 4H, Ar-H). 7.35 and 7.75 (2d of AA'BB' system, *J* = 8.5 Hz, 4H, Ar-H). Low-resolution mass spectrometry electrospray ionization (ESI+): 337.3 [M+Na].

5.3. Radiochemistry

[¹¹C]CO₂ was produced by the ¹⁴N(p,α)¹¹C nuclear reaction on a IBA CYCLONE 18/9 cyclotron. The synthesis was carried out in a

remotely controlled synthesis apparatus by Nuclear Interface (Münster). [¹¹C]Methyl iodide was prepared according to Crouzel and co-workers.³⁷ Radio-HPLC analyses were carried out with Discovery C18 column (Supelco 4.6 × 150 mm, 5 μm) using an indicated isocratic eluent with a flow rate of 1.0 ml/min. The products were monitored by an UV detector L4500 (Merck-Hitachi) at 240 nm and by γ-detection with a scintillation detector GABI (X-RAYTEST).

5.3.1. 1-[¹¹C]Methoxy-4-(2-(4-(methanesulfonyl)phenyl)-cyclopent-1-enyl)-benzene [¹¹C]**5**

[¹¹C]Methyl iodide was transferred in a stream of nitrogen into the reaction vessel containing phenol **6** (1.0 mg) in DMF (400 μL) and 5 N NaOH (30 μL) at room temperature. The formation of the corresponding phenolate occurred in situ immediately after the addition of NaOH to compound **6** at room temperature. After completion of the [¹¹C]methyl iodide transfer, the reaction vessel was sealed and heated at 60 °C for 3 min. The reaction mixture was diluted with eluent (1 mL), and the mixture was transferred from the reaction vessel onto a semi-preparative C-18 column (Nucleodur ISIS, Macherey-Nagel, C18, 250 × 10 mm, 5 μm) using CH₃CN/H₂O (70:30) as the mobile phase at a flow rate of 5 mL/min. The desired product eluted between 8 and 9 min. The fraction containing the ¹¹C-labeled compound [¹¹C]**5** was diluted with 30 ml of water and passed through a SPE-cartridge RP-18E (40–63 μm). The product was eluted from the cartridge with EtOH (1 mL), and the final product solution was prepared by the addition of isotonic sodium chloride (0.9%) solution (9.0 mL). An aliquot was taken for quality control using radio-HPLC (SPELCO Discovery C18, 150 mm × 4.6 mm, 5 μm, acetonitrile/water (70:30), flow rate: 1 ml/min, *t_R* = 5.1 min). Compound [¹¹C]**5** was obtained in 19% decay-corrected radiochemical yield (based upon [¹¹C]CO₂). The radiochemical purity exceeded 95%, and the specific activity was determined to be 20–25 GBq/μmol at the end-of-synthesis.

5.4. Cell uptake studies

Uptake experiments for *in vitro* evaluation of compound [¹¹C]**5** were performed in the following cells: THP-1 (human monocyte/macrophage line; DSMZ ACC 16), RAW 264.7 (mouse monocyte/macrophage line; ATCC TIB-71), NIH 3T3 (mouse fibroblast line; ECACC 93061524), 3T3-L1 (mouse preadipocyte (fibroblast-like) line; ECACC 86052701), FaDu (human head and neck squamous cell carcinoma line; ATCC HTB-43), and HT-29 (human colorectal adenocarcinoma line; ATCC HTB-38). Cells were routinely cultivated in RPMI 1640 medium or McCoy medium (HT-29) supplemented with 10% (v/v) heat-inactivated fetal calf serum (FCS), penicillin (100 U/mL), streptomycin (100 μg/mL), and glutamine (2 mM) at 37 °C and 5% CO₂ in a humidified incubator. Proinflammatory stimulation (transformation to macrophages) of THP-1 and RAW 264.7 cells was performed by adding 64 nM phorbol myristate acetate (TPA) for 72 h. For the uptake studies, cells were seeded in 24-well plates at a density of 5 × 10⁴ cells/mL and grown to confluence. Unstimulated THP-1 suspension cells were centrifuged and resuspended in fresh RPMI medium containing 10% FCS in 24-well plates at a density of 5 × 10⁵ cells/mL. The cell tracer uptake experiments using compound [¹¹C]**5** (1 MBq/mL; specific activity at application time, 12.1 ± 2.1 GBq/μmol) were performed in quadruplicate in medium both at 4 and 37 °C for 5, 10, 15, 30, 45, and 60 min. For blocking studies, the cells were preincubated for 10 min with a 100 μmol/L solution of the corresponding nonradioactive reference compound **5**. After the tracer uptake was stopped with 1 mL ice-cold PBS, the cells were washed three times with PBS and dissolved in 0.5 mL NaOH (0.1 M containing 1% (w/v) sodium dodecylsulfate). The radioactivity in the cell extracts was measured with a Cobra II gamma

counter (Canberra-Packard, Meriden, CT, USA). Total protein concentration in the samples was determined by the bicinchoninic acid method (BCA; Pierce, Rockford, Ill, USA) using bovine serum albumin as protein standard. Uptake data for all experiments are expressed as percent of injected dose per μg protein (%ID/ μg protein).

5.5. Biodistribution studies in rats

All animal experiments were carried out according to the guidelines of the German Regulations for Animal Welfare. The protocol was approved by the local Ethical Committee for Animal Experiments. The Wistar rats were housed under standard conditions with free access to standard food and tap water. Five animals (body weight 122 ± 16 g) for each time point were intravenously injected with approximately 20 MBq of [^{11}C]5 in 0.5 mL saline with 10% ethanol. Animals were sacrificed at 5 and 60 min post injection. Organs and tissues of interest were rapidly excised, weighed, and the radioactivity was determined using a Cobra II gamma counter (Canberra-Packard, Meriden, CT, USA). The activity in the selected tissues and organs was expressed as percent injected dose per gram tissue (%ID/g). The activity of the tissue samples was decay-corrected and calibrated by comparing the counts in tissue with the counts in aliquots of the injected tracer that had been measured in the gamma counter at the same time. Values are quoted as means \pm standard deviation (mean \pm SD) for a group of four animals.

5.6. Metabolite analysis

The radiotracer [^{11}C]5 was injected intravenously into male Wistar rats (30 MBq) or HT-29 tumor-bearing mice (20 MBq) under isoflurane (1.5%) oxygen anesthesia. Blood samples from the right femoral artery were taken using a catheter at 3, 5, 10, 30, and 60 min after injection. Plasma was separated by centrifugation (3 min, 11,000g) followed by precipitation of the plasma proteins with ice-cold methanol (1.5 parts per 1 part plasma) and centrifugation (3 min, 11,000g), and the supernatants were analyzed by HPLC. The radio-HPLC system (Agilent 1100 series) applied for metabolite analysis was equipped with UV detection (210 nm) and an external radiochemical detector (Canberra-Packard, Radiomatic Flo-one Beta 150TR) with PET flow cell. Analysis was performed on a Zorbax 300SB-C18 (250×9.4 mm; $5 \mu\text{m}$) column with acetonitrile/water (70/30) as the eluent at a flow rate of 2 mL/min.

5.7. Small animal PET imaging

General anesthesia of tumor-bearing mice was induced with inhalation of 3% isoflurane in oxygen, and was maintained with 1.5% isoflurane in oxygen and subsequently fixed in prone position on the microPET[®] bed. In the PET experiments, 30 MBq of [^{11}C]5 in 0.5 mL of saline was administered intravenously as a bolus via a tail vein.

PET imaging [^{11}C]5 in HT-29 tumor-bearing mice was performed over 60 min with a microPET[®] P4 scanner (Siemens CTI Molecular Imaging Inc., Knoxville). Data acquisition was performed in 3D list mode. A transmission scan was carried out prior to the injection of [^{11}C]5 using a ^{137}Cs point source. Emission data were collected continuously for 60 min after injection of [^{11}C]5. The list mode data were sorted into 4 sinograms for the 30 min frames and for the dynamic study using a framing scheme of 12×10 , 6×30 , 5×300 , and 9×600 s frames. The data were attenuation corrected and the static 30 min frames (30 to 60 min p.i.) were reconstructed by filtered back projection using a ramp filter. The pixel size was 0.949 by

0.949 by 1.212 mm and the resolution was around 1.85 mm. No correction for recovery and partial volume effects was applied. The image files were processed using the ASIPro software (SIEMENS, CTI Concorde Microsystems Inc., Knoxville) and the ROVER software (ABX medical software development, Radeberg, Germany). A summed image from 30 to 60 min p.i. was used to define the regions of interest (ROI). The data were normalized to the injected radioactivity by using ^{11}C standards from the injection solution measured in a γ -well counter (Isomed 2000, Germany) cross calibrated to the PET scanner and expressed in percent of injected dose per cubic centimeter (%ID/ cm^3). In the blocking experiments, compound 5 (5 mg/kg body weight) was injected intraperitoneally 10 min prior to radiotracer application.

Acknowledgments

The authors are grateful to Mareike Barth, Regina Herrlich, Andrea Suhr, Stephan Preusche, and Tilow Krauss for their excellent technical assistance.

References

- Kurumbail, R. G.; Kiefer, J. R.; Marnett, L. J. *Curr. Opin. Struct. Biol.* **2001**, *11*, 752–760.
- Marnett, L. J. *Curr. Opin. Chem. Biol.* **2000**, *4*, 545–552.
- Fitzpatrick, F. A. *Curr. Pharm. Des.* **2004**, *10*, 577–588.
- Warner, T. D.; Mitchell, J. A. *Proc. Natl. Acad. Sci. U.S.A.* **2002**, *99*, 13371–13373.
- Picot, D.; Loll, P. J.; Garavito, R. M. *Nature* **1994**, *367*, 243–249.
- Luong, C.; Miller, A.; Barnett, J.; Chow, J.; Ramesha, C.; Browner, M. F. *Nat. Struct. Biol.* **1996**, *3*, 927–933.
- Marnett, L. J.; Rowlinson, S. W.; Goodwin, D. C.; Kalgutkar, A. S.; Lanzo, C. A. *J. Biol. Chem.* **1999**, *274*, 22903–22906.
- Smith, W. L.; Garavito, R. M.; DeWitt, D. L. *J. Biol. Chem.* **1996**, *271*, 33157–33160.
- Herschman, H. R. *Biochim. Biophys. Acta* **1996**, *1299*, 125–140.
- Smith, W. L. In *Handbook of Eicosanoids: Prostaglandins and Related Lipids*; Willis, A. L., Ed.; CRC Press: Boca Raton, FL, 1987; pp 175–184.
- Herschman, H. R. *Biochim. Biophys. Acta* **1996**, *1299*, 125–140.
- Xu, X. C. *Anticancer Drugs* **2002**, *13*, 127–137.
- Jiménez, P.; García, A.; Santander, S.; Piazuolo, E. *Curr. Pharm. Des.* **2007**, *13*, 2261–2273.
- Brown, J. R.; DuBois, R. N. *J. Clin. Oncol.* **2005**, *23*, 2840–2855.
- de Vries, E. F.; van Waarde, A.; Buursma, A. R.; Vaalburg, W. *J. Nucl. Med.* **2003**, *44*, 1700–1706.
- McCarthy, T. J.; Sheriff, A. U.; Graneto, M. J.; Talley, J. J.; Welch, M. J. *J. Nucl. Med.* **2002**, *43*, 117–124.
- Prabhakaran, J.; Underwood, M. D.; Parsey, R. V.; Arango, V.; Majo, V. J.; Simpson, N. R.; Van Heertum, R.; Mann, J. J.; Kumar, J. S. *Bioorg. Med. Chem.* **2007**, *15*, 1802–1807.
- Wuest, F.; Höhne, A.; Metz, P. *Org. Biomol. Chem.* **2005**, *3*, 503–507.
- Majo, V. J.; Prabhakaran, J.; Simpson, N. R.; Van Heertum, R. L.; Mann, J. J.; Kumar, J. S. *Bioorg. Med. Chem. Lett.* **2005**, *15*, 4268–4271.
- de Vries, E. F.; Doorduyn, J.; Dierckx, R. A.; van Waarde, A. *Nucl. Med. Biol.* **2008**, *35*, 35–42.
- Toyokuni, T.; Kumar, J. S.; Walsh, J. C.; Shapiro, A.; Talley, J. J.; Phelps, M. E.; Herschman, H. R.; Barrio, J. R.; Satyamurthy, N. *Bioorg. Med. Chem. Lett.* **2005**, *15*, 4699–4702.
- Fujisaki, Y.; Kawamura, K.; Wang, W. F.; Ishiwata, K.; Yamamoto, F.; Kuwano, T.; Ono, M.; Maeda, M. *Ann. Nucl. Med.* **2005**, *19*, 617–625.
- Tian, H.; Lee, Z. J. *Label. Compd. Radiopharm.* **2006**, *49*, 583–593.
- Tanaka, M.; Fujisaki, Y.; Kawamura, K.; Ishiwata, K.; Qinggeletu; Yamamoto, F.; Mukai, T.; Maeda, M. *Biol. Pharm. Bull.* **2006**, *29*, 2087–2094.
- Yang, D. J.; Bryant, J.; Chang, J. Y.; Mendez, R.; Oh, C. S.; Yu, D. F.; Ito, M.; Azhdarinia, A.; Kohanim, S.; Edmund Kim, E.; Lin, E.; Podoloff, D. A. *Anticancer Drugs* **2004**, *15*, 255–263.
- Kabalka, G. W.; Mereddy, A. R.; Schuller, H. M. *J. Label. Compd. Radiopharm.* **2005**, *48*, 295–300.
- Reitz, D. B.; Li, J. J.; Norton, M. B.; Reinhard, E. J.; Collins, J. T.; Anderson, G. D.; Gregory, S. A.; Koboldt, C. M.; Perkins, W. E.; Seibert, K., et al. *J. Med. Chem.* **1994**, *37*, 3878–3881.
- Li, J. J.; Anderson, G. D.; Burton, E. G.; Cogburn, J. N.; Collins, J. T.; Garland, D. J.; Gregory, S. A.; Huang, H. C.; Isakson, P. C.; Koboldt, C. M., et al. *J. Med. Chem.* **1995**, *38*, 4570–4578.
- Bagga, D.; Wang, L.; Farias-Eisner, R.; Glaspy, J. A.; Reddy, S. T. *Proc. Natl. Acad. Sci. U.S.A.* **2003**, *100*, 1751–1756.

30. Goppelt-Struebe, M.; Schaefer, D.; Habenicht, A. J. *Br. J. Pharmacol.* **1997**, *122*, 619–624.
31. Mbonye, U. R.; Wada, M.; Rieke, C. J.; Tang, H. Y.; Dewitt, D. L.; Smith, W. L. *J. Biol. Chem.* **2006**, *281*, 35770–35778.
32. Lev-Ari, S.; Strier, L.; Kazanov, D.; Madar-Shapiro, L.; Dvory-Sobol, H.; Pinchuk, I.; Marian, B.; Lichtenberg, D.; Arber, N. *Clin. Cancer Res.* **2005**, *11*, 6738–6744.
33. Yan, H.; Kermouni, A.; Abdel-Hafez, M.; Lau, D. C. *J. Lipid Res.* **2003**, *44*, 424–429.
34. Murakami, A.; Takahashi, D.; Kinoshita, T.; Koshimizu, K.; Kim, H. W.; Yoshihiro, A.; Nakamura, Y.; Jiwajinda, S.; Terao, J.; Ohigashi, H. *Carcinogenesis* **2002**, *23*, 795–802.
35. Haase, C.; Bergmann, R.; Oswald, J.; Zips, D.; Pietzsch, J. *Anticancer Res.* **2006**, *26*, 3527–3533.
36. Herschman, H. R.; Talley, J. J.; DuBois, R. *Mol. Imaging Biol.* **2003**, *5*, 286–303.
37. Crouzel, C.; Langström, B.; Pike, V. W.; Coenen, H. H. *Appl. Radiat. Isot.* **1987**, *38*, 601–603.
38. Mestre, J. R.; Mackrell, P. J.; Rivadeneira, D. E.; Stapleton, P. P.; Tanabe, T.; Daly, J. M. *J. Biol. Chem.* **2001**, *276*, 3977–3982.
39. Kuge, Y.; Katada, Y.; Shimonaka, S.; Temma, T.; Kimura, H.; Kiyono, Y.; Yokota, C.; Minematsu, K.; Seki, K.; Tamaki, N.; Ohkura, K.; Saji, H. *Nucl. Med. Biol.* **2006**, *33*, 21–27.
40. Harris, R. C. *J. Am. Soc. Nephrol.* **2000**, *11*, 2387–2394.
41. Koki, A. T.; Masferrer, J. L. *Cancer Control* **2002**, *9*, 28–35.
42. Hwang, J. T.; Kim, Y. M.; Surh, Y. J.; Baik, H. W.; Lee, S. K.; Ha, J.; Park, O. *J. Cancer Res.* **2006**, *66*, 10057–10063.
43. Sano, H.; Kawahito, Y.; Wilder, R. L.; Hashiramoto, A.; Mukai, S.; Asai, K.; Kimura, S.; Kato, H.; Kondo, M.; Hla, T. *Cancer Res.* **1995**, *55*, 3785–3789.
44. Kargman, S. L.; O'Neill, G. P.; Vickers, P. J.; Evans, J. F.; Mancini, J. A.; Jothy, S. *Cancer Res.* **1995**, *55*, 2556–2559.
45. Petersen, S.; Haroske, G.; Hellmich, G.; Ludwig, K.; Petersen, C.; Eicheler, W. *Anticancer Res.* **2002**, *22*, 1225–1230.
46. Wang, L.; Chen, W.; Xie, X.; He, Y.; Bai, X. *Exp. Oncol.* **2008**, *30*, 42–51.
47. Still, W. C.; Kahn, M.; Mitra, A. *J. Org. Chem.* **1978**, *43*, 2923–2925.